

An analytical description of rate effects in timing RPCs

D. González-Díaz ^{a*}, P. Fonte ^{b c}, J. A. Garzón^a, A. Mangiarotti ^d

^aLabCaF, Departamento de Física de Partículas, Universidade de Santiago de Compostela, 15782, Santiago de Compostela, Spain

^bLIP, Departamento de Física, Universidade de Coimbra, 3004-516, Coimbra, Portugal

^cInstituto Superior de Engenharia de Coimbra, Rúa Pedro Nunes, 3030-199, Coimbra, Portugal

^dPhysikalisches Institut der Universität Heidelberg, Philosophenweg 12, D-69120, Heidelberg, Germany

An analytical framework for describing the RPC behavior under high irradiation is proposed, including the effect of the fluctuations of the field. The description is compared with an equivalent MC and data for timing RPCs, showing good agreement. Moreover, the formalism allows to clearly identify the main variables ruling the process.

By using the DC electric properties of the plates, the MC allows to reproduce the charging-up process in a dynamic situation, revealing that it takes place at the scale of the relaxation time, varying with the primary rate.

1. INTRODUCTION

A first attempt to describe the RPC behavior at high rates including the electric properties of the plates has been recently performed [1], despite the difficulties of such an enterprise are not negligible (see [2] for phenolic plates or [3] for float glass).

Moreover, different ‘high rate RPC’ technologies are emerging, not being based on Bakelite or glass electrodes [4], [5], and still the only available analytical description of ‘rate effects’ is based on a simple DC model ([6], for instance):

$$\bar{V}_{drop} = V - \bar{V}_{gap} = \bar{I}R = \bar{q}\phi\rho d \quad (1)$$

that relates the average voltage drop \bar{V}_{drop} at high rates $\phi[\text{L}^{-2} \text{T}^{-1}]$ with the ohmic drop in the resistive plates, namely $\bar{I}R$. The current \bar{I} is proportional to the average charge per avalanche (\bar{q}), that is ruled, expectedly, by the average voltage in the gap \bar{V}_{gap} , thus yielding:

$$\bar{V}_{gap} = \bar{V}_{gap}(V, \phi\rho d) \quad (2)$$

being ρ the resistivity of the plate and d its thickness. As long as a certain observable depends only

on the average field in the gap, the DC model can be applied ([8], [9] for instance), predicting an increase of the maximum attainable rates proportional to the decrease of the ‘column resistivity’ ρd .

In particular, the fluctuations of V_{gap} , the role of the relative dielectric permittivity ϵ_r of the plates, and the area A affected per avalanche are absent in the DC description.

2. DC MODEL AND DATA

Data for timing RPCs at high rates, taken from [10], have been analyzed under the following cuts:

1. Particles with $\beta > 0.75c$ (c the speed of light), close to the MIP dip, are selected.
2. The electronic contribution to the time resolution is reduced by purging events with $q_{prompt} < 200 \text{ fC}$ (see [11]).
3. Events within the first 2 ‘in-spill’ seconds are removed, guaranteeing a *stationary situation* of the field in the gap (see section 3).

*Corresponding author. diego@fpddux.usc.es

4. The detector efficiency is corrected for the geometric inefficiency estimated in [10].

The DC model allows to obtain $\bar{V}_{gap}(V, \phi \rho d)$ as described in [7], [8], by assuming [12]:

$$\bar{q} = a(\bar{V}_{gap} - V_{th}) \quad (3)$$

characteristic of the Space-Charge regime. Expression 3 together with eq. 1, results in:

$$\bar{V}_{gap} = V_{th} + \frac{(V - V_{th})}{1 + a\phi\rho d} \quad (4)$$

Here, the attention is focused on the time distribution through the time at maximum t_o and resolution σ_T , and on the efficiency ε . These magnitudes can be parameterized from theoretical considerations [11] and semi-empirically [13], respectively:

$$t_o(\bar{V}_{gap}) = \frac{1}{S(\bar{V}_{gap})} \ln \frac{m_t}{-\ln(1 - \varepsilon(\bar{V}_{gap}))} \quad (5)$$

$$\sigma_T(\bar{V}_{gap}) = \frac{K[\varepsilon(\bar{V}_{gap})]}{S(\bar{V}_{gap})} \quad (6)$$

$$\varepsilon(\bar{V}_{gap}) = \frac{\varepsilon_o}{1 + e^{-\theta(\bar{V}_{gap} - V_{ref})}} \quad (7)$$

where the identification $V_{gap} \rightarrow \bar{V}_{gap}$ (DC model) has been performed. The constants ε_o , θ and V_{ref} regulate the efficiency behavior and the parameterization of K as a function of the intrinsic efficiency ε can be found in [11]. m_t is the charge necessary to fire the comparator threshold in units of the electron charge and the growth coefficient $S = \alpha^* v_d$ has been measured following [14], yielding:

$$S[\text{ns}^{-1}] = (6.0 \pm 1.2)V_{gap}[\text{kV}] - 7.2 \pm 3.1 \quad (8)$$

for the gas mixture used in [10] and $V_{gap} > 2.4$ kV.

A fit to t_o and ε data was performed, providing the values of $a=2.9$ pC/kV and $V_{th}=2.1$ kV, that are used in expression 6 for σ_T , without any extra assumption. The proposed description is compared with data in figs. 1 (fitted) and 2 (non-fitted).

The overall good agreement with the DC model suggests that the fluctuations of the voltage have little influence over the RPC performances, once

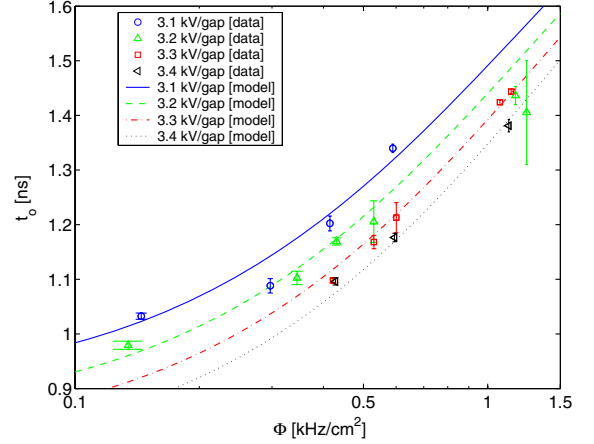


Figure 1. Time at maximum t_o fitted to the DC model. The efficiency ε was also included in the global fit, but is not shown (see [15] for details).

the stationary situation has been reached (i.e: the plates are charged-up). The implications of these observations are discussed in the following.

3. ANALYTICAL DESCRIPTION OF THE FLUCTUATIONS

Being the time resolution σ_T a second moment of the RPC time response, it is expected to be tightly related to the fluctuations of the voltage across the gap. Fortunately, once σ_T is expressed analytically (eq. 6), the influence of small fluctuations on the variables can be estimated easily [16]:

$$\text{rms}_T^2 = \left[\frac{K^2}{S^2} + t_o^2 \left(\frac{E}{S} \frac{dS}{dE} \right)^2 \left(\frac{\text{rms}_E}{E} \right)^2 \right]_{\bar{E}_{gap}} \quad (9)$$

where the presence of non-Gaussian timing tails has been neglected ($\bar{t} \simeq t_o$). It has been assumed that rms_E (fluctuations of the field) and K/S (intrinsic avalanche fluctuations) are decoupled, and that $\frac{1}{St} \frac{dSt}{dE} \ll \frac{1}{S} \frac{dS}{dE}$, as is reasonable under typical timing RPC operating conditions.

Eq. 9 can be used for evaluating the effects arising from *static* fluctuations due to non-

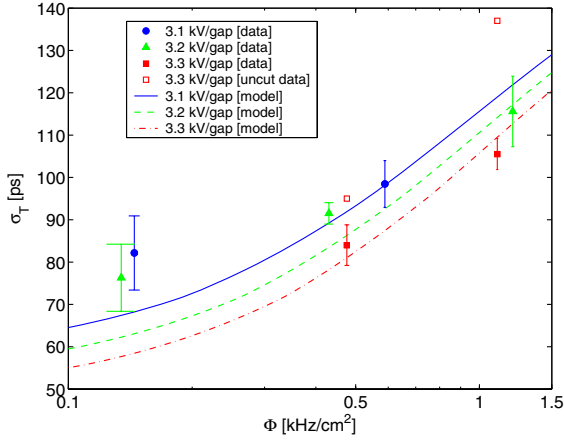


Figure 2. Set of data for σ_T with improved statistical significance (each point was obtained from the average over more than two runs) and DC model (lines, non-fitted). Open points stand for the time resolution including the first 2 seconds (charging-up time of the plates).

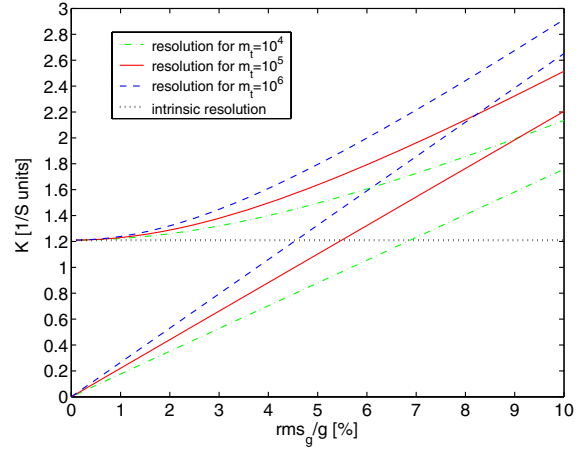


Figure 3. Influence of the mechanic inaccuracies (rms_g/g) on the time resolution (in units of $1/S$), for a 1-gap timing RPC under typical conditions. The straight lines indicate the contribution of the mechanics and the curved ones stand for the total resolution. This figure must replace the published Fig. 2 in [16], as the reader can check.

uniformities of the gap size g ($\bar{E}_{gap} = E$, $\frac{\text{rms}_E}{E} = \frac{\text{rms}_g}{g}$). The expectation for a typical 1-gap timing RPC is presented in fig. 3 ($V = 3.2$ kV, $S = 11$ ns $^{-1}$, $dS/dV = 6.6$ ns $^{-1}$ kV $^{-1}$, $\varepsilon = 78\%$). It is shown the intrinsic resolution (rms) obtained from formula 6 (dotted) and the contribution due to mechanics (straight lines), together with the total resolution obtained from the evaluation of eq. 9 (curved lines). A worsening by 20% on the time resolution for fluctuations in the gap size above 4% is predicted, with the usual threshold $m_t \sim 10^5$.

Remarkably, eq. 9 describes also the effect of *dynamic* fluctuations of the field caused by avalanches. In particular, the assumption that $\text{rms}_{E_{gap}}$ and K/S are decoupled still holds, due to the different time scales involved in charge flow (the relaxation time of the glass is \sim s) and avalanche fluctuations (\sim ns).

The problem in a dynamic situation is more how to get an analytical expression for $\text{rms}_{E_{gap}}$, a step accomplished through the following model:

1. The region illuminated by a single avalanche is assimilated to an area A , that is referred as the *influenced area* per avalanche [1].
2. Each RPC gap is represented by the equivalent circuit shown in fig. 4.
3. The charge released by the avalanches is given by a sum of shots q_k at the gap capacitance. As the avalanche drift times are much smaller than the relaxation time of the glass, the shots are considered as instantaneous for the description of the latter process.

Under these assumptions, the RPC behavior can be described by a simple RC circuit, where the current generated by the avalanches and the voltage drop are given by:

$$I(t) = \sum_k q_k \delta(t - t_k) \quad (10)$$

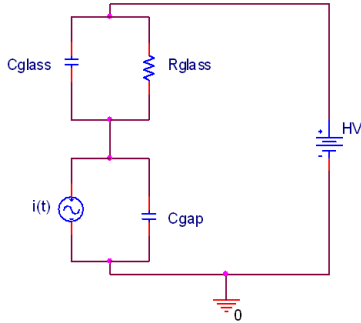


Figure 4. Equivalent circuit for a 1-gap RPC consisting of aluminum and glass electrodes.

$$V(t) = \sum_k \frac{q_k}{C_{glass} + C_{gap}} e^{-\frac{t-t_k}{\tau_g}} \Theta(t-t_k) \quad (11)$$

and:

$$\tau_g = R(C_{glass} + C_{gap}) = \rho \epsilon_o \left(\epsilon_r + \frac{d}{g} \right) \quad (12)$$

is the RPC relaxation time. From the measured DC values, $\rho = 6.5 \cdot 10^{12} \Omega \text{cm}$ ($T = 25^\circ \text{C}$) and preliminary estimates of $\epsilon_r = 6$, a value $\tau_g \simeq 5 \text{ s}$ is obtained.

The fluctuations of $V(t)$ can be evaluated through the Campbel theorem (see [17]) as:

$$\text{rms}_{V_{gap}}^2 = \frac{\rho^2 d^2 \phi}{2\tau_g A} \bar{q}^2 \left(1 + \frac{\text{rms}_q^2}{\bar{q}^2} \right) \quad (13)$$

in the absence of shot-to-shot correlations. Such correlation can be introduced, in average, by recalling the relation between \bar{q} and ϕ (eqs. 3, 4) and taking the parameters a and V_{th} from section 2. The resulting description is denoted as ‘Campbel theorem with drop’ in the following, and, remarkably, contains all the information of the shape of the charge spectra in a single parameter, rms_q/\bar{q} .

The accuracy of the analytical description is checked by a MC simulation that includes the correlation shot by shot. For illustration, three characteristic charge distributions are considered in

simulation: $dN/dq \sim 1$, $dN/dq \sim 1/q$, $dN/dq \sim e^{-q}$, defined such that $\text{rms}_q/\bar{q} = 0.6$. The shape of dN/dq is assumed to be independent from the field, in agreement with the uniform value of $\text{rms}_q/\bar{q} = 0.7$ observed for the prompt charge [15] (in 4 gaps, therefore $\text{rms}_q/\bar{q} = 1.4$ per gap). The MC and analytical solutions are compared under stationary conditions in fig. 5 ($A = 1 \text{ mm}^2$).

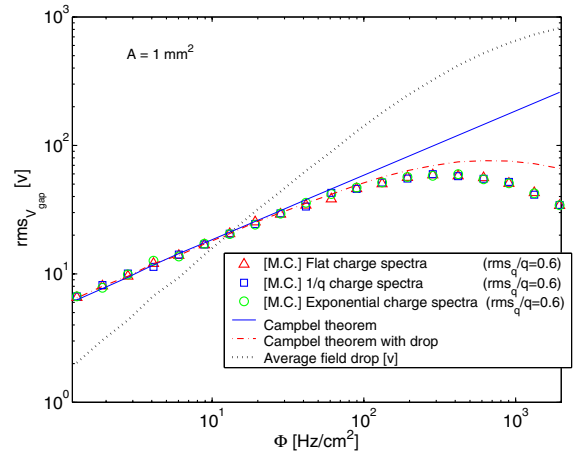


Figure 5. Fluctuations of the voltage ($\text{rms}_{V_{gap}}$) for the proposed analytic descriptions (full line, dot-dashed line) together with MC calculations for different charge spectra.

Due to the average description of the correlation between shots, discrepancies up to a factor of 2 are present at the highest rates considered. Despite this, a relevant scaling property is common to both the analytical and MC solutions:

$$\frac{\text{rms}_{V_{gap}}}{\bar{V}_{drop}} \sim \sqrt{\frac{\left(1 + \frac{\text{rms}_q^2}{\bar{q}^2} \right)}{2\bar{N}}} \quad (14)$$

The higher the average number of shots contributing per influenced region $\bar{N} = A\phi\tau_g$, the smaller is the contribution of the fluctuations.

With $\text{rms}_{V_{gap}}$ obtained from the exact MC, eq. 9 can be used for constraining the value of A

($\text{rms}_{E_{gap}} = \text{rms}_{V_{gap}}/g$). An approximation to the multi-gap situation is done by assuming that all the gaps are uncorrelated and contribute the same to σ_T . The results shown in fig. 6 indicate that $A < 0.3 \text{ mm}^2$ is at odds with data, while estimates of this magnitude from electrostatic calculations [18] point to values at the scale of mm^2 .

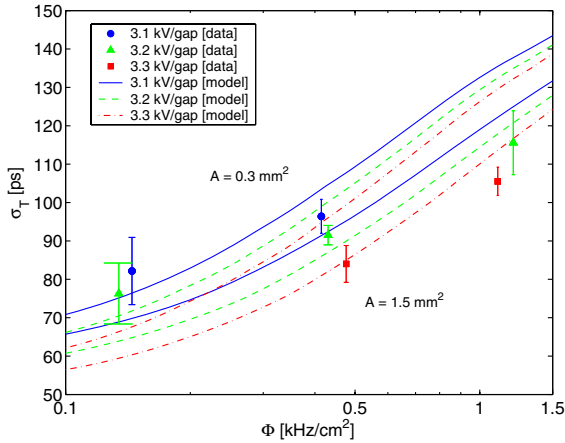


Figure 6. Data and model for two different values of the influenced area A ($\text{rms}_q/\bar{q} = 1.4$ per gap).

4. THE CHARGING-UP TIME

The charging-up time (t_{eq}) can be defined in a natural way as the time it takes to the RPC to reach a stationary situation, whenever a certain amount of charge is released over the surface of its resistive plates. If this happens as a consequence of the application of HV, the time scale of the process is, in fact, the relaxation time of the plates. A similar effect occurs when the irradiation over the RPC starts suddenly. In that case, simple considerations lead to the expression [15]:

$$t_{eq}(\tau_g, \rho d) = \frac{\tau_g}{a\phi\rho d} \ln(1 + a\phi\rho d) \quad (15)$$

by assuming an accumulation of shots with average rate ϕ , whose charge is correlated as described

by eq. 3.

The charging-up process according to M.C. is illustrated in fig. 7 (up). Thus, t_{eq} can be defined as the time it takes to reach a certain fraction f of the voltage drop corresponding to the stationary situation:

$$\bar{V}_{drop}(t_{eq}) = \lim_{k \rightarrow \infty} \sum_{i=1}^k \frac{V_{drop,i}(t_{eq})}{k} = f\bar{V}_{drop}(\infty) \quad (16)$$

where the stationary value $\bar{V}_{drop}(\infty)$ coincides with the value obtained from the DC model (eq. 4) and the sum runs over an infinite number of cells. For convenience, f is defined so that $f = 1 - 1/e = 63\%$, yielding $t_{eq} = \tau_g$ in the low rate limit. With such a prescription, the stabilization time can be evaluated for different rates and values of the influenced area. The behavior of the stabilization time is shown in fig. 7, being in qualitative agreement with the measurement of Ref. [3] (decreasing at high rates) and does not depend substantially on the influenced area. The decreasing behavior is a consequence of the fact that the maximum voltage drop achievable in the gap is roughly limited to the value $V - V_{th}$ while the rate can grow indefinitely, reducing the average time necessary to reach such situation.

In data, the charging-up process shows up as drifts on the RPC observables as a function of the time within the spill. In particular, the average prompt charge decreases (lower gains) while the formation time of the signal increases. Aiming at comparing with data, the expected behavior of $\bar{V}_{drop}(t)$ was determined from MC (fig. 7, up) so that $t_o[\bar{V}_{gap}(t)]$ can be predicted by using eq. 5. For obtaining the best agreement, a value of $\epsilon_r \simeq \frac{1}{3}\epsilon_r(\text{DC})$ was assumed, corresponding to $\tau_g \simeq 2.5 \text{ s}$ (fig. 8). In fact, as the stabilization time does not depend on A and all the parameters are constrained by data (section 2), the comparison shown in fig. 8 depends only on the relative dielectric permittivity, ϵ_r . The observed discrepancy points to the need of more theoretical efforts.

5. CONCLUSIONS

A framework for describing analytically the behavior of RPCs at high illumination has been introduced and compared with MC, allowing to

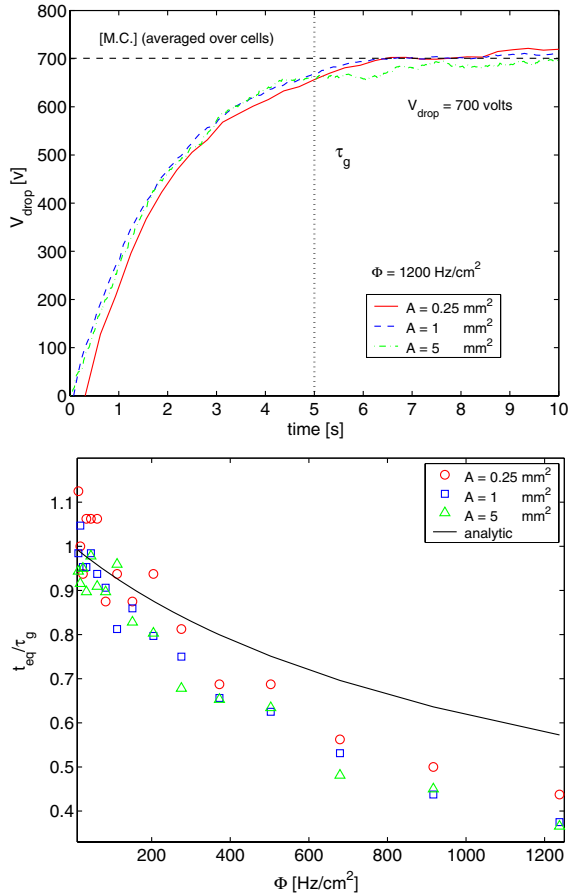


Figure 7. Up: average behavior of $\bar{V}_{drop}(t)$. Down: stabilization time t_{eq} as a function of rate, normalized to the relaxation time τ_g (MC). Different values of A are considered. Eq. 15 is also shown (line).

identify the main variables ruling the phenomena, namely, ρd (ohmic drop of the applied voltage), $A\tau_g$ (fluctuations of the electric field) and τ_g (charging-up time of the plates). The model has been applied to data from tRPCs, showing a good agreement within a simple DC model, thus constraining A (the influenced area per avalanche) to be larger than 0.3 mm^2 .

The MC describes the charging-up process,

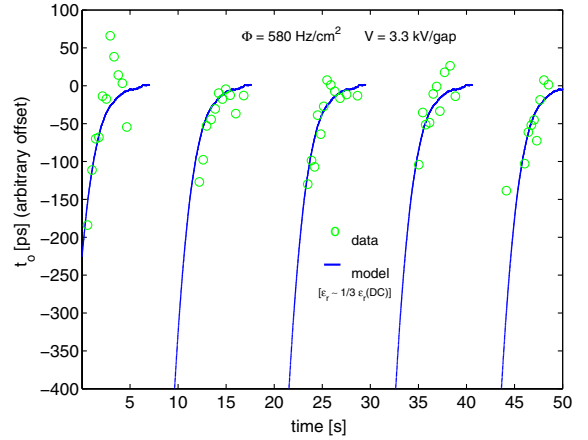


Figure 8. Behavior of t_o as a function of the irradiation time, obtained by using together eq. 5 and $\bar{V}_{drop}(t)$ from MC. Open circles show data corresponding to the mean value of the time distribution \bar{t} (averaged over 200 shots).

showing that it takes place at a time scale of the order of the relaxation time (τ_g) of the RPC. Such effect explains naturally the overestimation on rate capabilities reported for short spills [19].

If further work confirms the negligible impact of the fluctuations of V_{gap} in timing, it would open the possibility of over-biasing the voltage in the chamber at high rates. The feasibility of such approach must, however, be considered with care: in the present case, the voltage drop at $V = 3.2 \text{ kV}$, $\Phi = 1200 \text{ Hz/cm}^2$, is as low as $\bar{V}_{drop} \simeq 0.7 \text{ kV}$ requiring, however, an over-voltage as large as $\Delta V = 2.5 \text{ kV}$ (around 3 times the actual drop) for keeping \bar{V}_{gap} at 3.2 kV . Such over-voltage must take into account, eventually, the charging-up time.

ACKNOWLEDGEMENTS

This work was co-financed by MCYT FPA2000-2041-C02-02, FPA2003-7581-C02-02, XUGA PGIDT-02-PXIC-20605-PN, the EU 6th FP contract RII3-CT-2003-506078, FEDER and

FCT POCI/FP/63411/2005.

DGD acknowledges the hospitality received at the University of Heidelberg, to W. Riegler for discussions on the interpretation of A , and to J. Lamas-Valverde who suggested to look at the in spill structure. The part on fluctuations is strongly inspired on discussions of the authors with M. Abbrescia.

REFERENCES

1. M. Abbrescia, Nucl. Instr. and Meth. A 533(2004)7.
2. I. Crotty et al., Nucl. Instr. and Meth. A 337(1994)370.
3. M. Fraga et al., Nucl. Instr. and Meth. A 419(1998)485.
4. L. Lopes et al., Nucl. Instr. and Meth. A 533(2004)69.
5. L. Lopes et al., in these proceedings.
6. G. Aielli et al., Nucl. Instr. and Meth. A 456(2000)82.
7. G. Carboni et al., Nucl. Instr. and Meth. A 498(2003)135.
8. D. González-Díaz et al., Nucl. Instr. and Meth. A 555(2005)72.
9. C. Gustavino et al., Nucl. Instr. Meth. A 533(2004)116.
10. H. Alvarez-Pol et al., Nucl. Instr. and Meth. A 535(2004)277.
11. A. Mangiarotti et al., Nucl. Instr. and Meth. A 533(2004)16.
12. G. Aielli et al., Nucl. Instr. Meth. A 508(2003)6.
13. M. Alvigi et al., Nucl. Instr. Meth. A 518(2004)79.
14. A. Blanco et al., IEEE Trans. Nucl. Sci. 48(2001)1249.
15. D. González-Díaz, Ph.D. Thesis, USC, 2006.
16. A. Blanco et al. Nucl. Instr. and Meth. A 535(2004)272.
17. P. W. Nicholson, “Nuclear Electronics”, John Wiley & Sons, 1974.
18. C. Lippmann et al., in these proceedings.
19. P. Colrain et al., Nucl. Instr. and Meth. 456(2000)62.